Detection of Multitransition Abrupt Changes in Multitemporal SAR Images

Ozan Dogan and Daniele Perissin

***Abstract*—This paper addresses the detection of abrupt and stepwise changes in multitemporal sequences of synthetic aperture radar (SAR) images. Specifically, the major motivation is to deal with the change detection of urban features with multitemporal step patterns. In contrast to most techniques presented in the past, that only use couples of adjacent images, in this work multi-SAR images are used for the change detection purpose. The proposed method is appropriate for the generation of new SAR satellite systems that has a high revisit time, generating many successive image of the same area. We attacked on two aspects of the problem: detection of multitransition instants (TIs) of the SAR amplitude time series and detection of the probable changes. For this purpose, the analysis of variance (ANOVA), technique is used. ANOVA achieves a representation of the relation of all group changes. The features extracted by ANOVA are utilized for the supervised classification procedure. The proposed technique provides promising results for the classification of abrupt changes like in urban areas.**

***Index Terms*—Analysis of variance (ANOVA), change detection, synthetic aperture radar (SAR), time-series analysis.**

I. Introduction

URBAN area change detection is an important topic that has many applications, such as damage assessment, land usage awareness, land abuse detection, etc. There are many works in the literature using a pair of synthetic aperture radar (SAR) images for the change detection application [1]–[10]. These methods are mostly taking into account only a couple of images of the same scene. The comparison of that much limited number of observations suffers heavily from the corruption of independent random processes such as the system noise, atmospheric effects, image misregistration, and radiometric and geometric distortions of the two images. It is obvious that increasing the number of observations and extending the data set to extract a time-series analysis will improve the change detection accuracy.

The availability of multitemporal SAR images gives the opportunity for time-series analysis techniques such as multitemporal image filtering [11], permanent scatterers (PSs) [12], temporal behaviour of the PSs [13], and classification of urban structures [14], due to the increased capability of imaging sensors. However, there is still little effort about the application of the state-of-the-art techniques to the multitemporal time series of SAR images within the change detection perspective.

Taking into consideration the time series of a pixel, one can observe at least four types of cases: abrupt changes (urban constructions, deforestration area [20], etc.), evolutionary changes (vegetation areas), no changed areas, i.e., stable areas (urban regions), and periodic changes (vegetation evolution according to seasons). For the urban area change detection problem, as it is the case in this work, the major motivation is to detect the abrupt changes.

In [18], in order to detect these abrupt changes, a maximum-likelihood approach is proposed assuming that the transition instants (TIs) are known, single and in the middle of the data set (to guarantee an equal number of groups). In order to relax these strict assumptions, in [19], the TIs are computed through maximizing the likelihood and the unequal number of groups are taken into account with a lower performance; keeping the single TI assumption. In [15], a multitemporal edge detection procedure is followed by a multitemporal change detection procedure. Although the proposed method utilizes multi-SAR images, change detection is applied to the two images that generates "the strongest temporal contrast," disregarding the opportunity of extracting a higher contrast between two different groups of SAR pixels of the same region. In [16], the most stable states of a pixel are taken as a reference in order to compare with the whole series of the data following a supervised classification and validation by using two simulated SAR images. However, in this case, the most of the temporal combinations are neglected and again, single and known TI assumption is still a problem.

Given a set of SAR images for the abrupt change detection purpose, two different criteria shall be considered: first, the TIs shall be localized. These TIs are not necessarily constant for each changed region of the whole image area but, as it is mostly the case, is varying region-by-region. Next, the number of TIs is allowed to be more than one. A single TI approach can be acceptable for a comparably low number of images (such as seven images in [15] or ten images in [18]); however, once the sequence is longer, forcing the region to only two states decreases the performance of the change detection technique. Second, the change detection must be applied to a group of data. Many state-of-the-art techniques are applied to detect a significant difference between two groups of data. Once the number of TIs is more than one and TIs are assumed to be localized, these methods can be applied to compare each group pairs separately. However, considering the whole data set promises more statistical features than comparing in pairs, results in

Manuscript received March 12, 2013; revised September 24, 2013; accepted November 12, 2013. The work was supported in part by CUHK funds and in part by Infoterra Beijing, which provided TerraSAR-X data over Hong Kong.

O. Dogan is with ORTANA, Ankara, Turkey (e-mail: ozan.dogan@be.itu.edu.tr).

D. Perissin is with the School of Civil Engineering, Purdue University, West Lafayette, IN 47907 USA (e-mail: perissin@purdue.edu).

Color versions of one or more of the figures in this paper are available online at http://ieeexplore.ieee.org.

Digital Object Identifier 10.1109/JSTARS.2013.2295357

better false alarm performance. This fact is also known to be the major motivation of the ANOVA over student's t-test.

In this work, we derive a method in order to process the whole sequence to optimally estimate the TIs of possible step patterns; then applied a further test to decide whether or not a step change must be detected. For this purpose, we proposed the ANOVA method that maximizes the ratio between the sum of squares between the groups and within the groups. Instead of comparing each couple of groups to detect a change, we utilized the ANOVA also for the change detection purpose in order to take the advantage of ANOVA's potentiality to express the relationship between and within groups. The outputs of ANOVA, F values, and TIs are used as features for a further classification procedure of the changes. This paper is organized as follows. Section II presents a detailed description of the problem definition. Section III is to discuss the change detection, localization of the TIs, and the classification. Section IV includes the verification and validation of the method with the application to a series of TerraSAR-X data of Chinese University of Hong Kong (CUHK).

II. Problem Formulation

The amplitude of radar images is affected by several factors including characteristics of the observed objects (such as material, shape, dimensions, etc.) and acquisition-related parameters (such as time, geometry, and temperature). The goal of SAR change detection in terms of monitoring is to detect meaningful structural changes of images whose amplitude is changed. In order to suppress the noise to distinguish the informative signals, statistical techniques are needed to be applied to a set of observations. This can be realized either comparing a statistically relevant set of pixels from two images (along the spatial dimension) or by comparing a single pixel in a statistically relevant set of images (along the time dimension).

In this paper, we start with analyzing the amplitude time series of a single pixel in an interval of observation and next classifying the changes. A reasonable number of images enable us to statistically analyze the temporal characteristics for each pixel.

Next is to formulate the problem: let G_i be a group of SAR images that are already coregistered to a preselected master image. A misregistration may be held in between the two images, but it is most likely to be detected as a change. The index $i = 0, 1, 2, \ldots, K-1$ represents the group number and K is the number of groups. The problem is to detect if there is a "statistically significant change" at instants of i's.

Let us assume that there is only one TI of a sequence of a pixel, as this is the case of the literature so far. Hence, there are two groups:

$G_1 = I_0, I_1, \ldots, I_k$ and $G_2 = I_{k+1}, I_{k+2}, \ldots, I_{N-1}$, where I_i is the amplitude of SAR images and N is the number of SAR images.

In this case, one can simply propose a t-test to evaluate the difference of the groups and assign a threshold by determining the probability of false alarm. Another approach can be fitting a likelihood estimator and a thresholding in order to detect the changes [14]. Also, a multitemporal edge detector that takes into account the ratio of group means can be a solution for this problem [11] as the abrupt changes mostly obey a strong mean difference. For the case where there are more than two groups $G_1, G_2, \ldots, G_M$, one can simply extent one of these methods by comparing the adjacent groups. However, in this case, the advantage of evaluating all the relations of the groups is not handled, yielding an increase in false alarm rate. Thus, a method that handles the difference of all the groups will be useful. Also the detection of the groups and localization of the instants shall be included in this method.

In order to show the characteristics of multitransition case, the time series of 70 TerraSAR-X images of CUHK, acquired during the end of 2008 to the middle of 2010, is observed and typical time series of three different pixels is shown in Fig. 1. From left to right, single, double, and four TIs can be observed for an amplitude time series.

There are two more typical changes that are observed especially in the vegetation areas: the first is the evolutionary one, where a gradual change is taken into account like the growth of the vegetation, whereas the second is the periodic changes like the seasonal changes. These two are out of the scope of this work as the major motivation is urban monitoring.

III. Methodology

In this work, the ANOVA technique is used in order to detect the changes. First, the possible TIs are estimated by maximizing the F values and second, the maximum F values and the variance of the instants are computed. These are given as input for the classification procedure.

A. Analysis of Variance

For a given test site, the collected radar reflectivity series can be divided into groups along time, at the instant of changes, in order to cover the abrupt changes. The ANOVA is a widely used statistical technique, especially in experimental result analysis. It simply deals with the ratio of the variances between the groups and within each group and rejects the zero hypothesis, meaning a change detection decision, when this ratio is high enough. For this application, the "observed variable" is the radar reflectivity and the "interested variable" is the step change due to the recently constructed object.

Next is to formulate ANOVA for the time-series analysis of SAR data. Given K independent observations of each size N_j

$$\begin{aligned} G_1 &= I_0, I_1, \ldots, I_{N_1-1} \\ G_2 &= I_{N_1}, I_{N_1+1}, \ldots, I_{N_2+N_1-1} \ldots \\ G_K &= I_{\sum_{k=1}^{K} N_i}, I_{\sum_{k=1}^{K} N_i+1}, \ldots, I_{N-1}. \end{aligned} \tag{1}$$

We would like to test the hypothesis that the means of all distributions are equal

$$H_0 : \mu_1 = \mu_2 = \cdots = \mu_K. \tag{2}$$

Under the null hypothesis H_0, one can define the F value as

$$F = \frac{N-K}{K-1} \frac{\sum_{j=1}^{K} N_j (\mu_j - \mu)^2}{\sum_{i=1}^{K} \sum_{k=1}^{N} (I_{ik} - \mu_k)^2} \sim F_{K-1,N-K} \tag{3}$$

with a distribution of $F_{K-1,N-K}$, μ is the mean of the whole data, μ_j's are the group means, and I_{ik} values are the amplitudes of the pixel corresponding to each group.

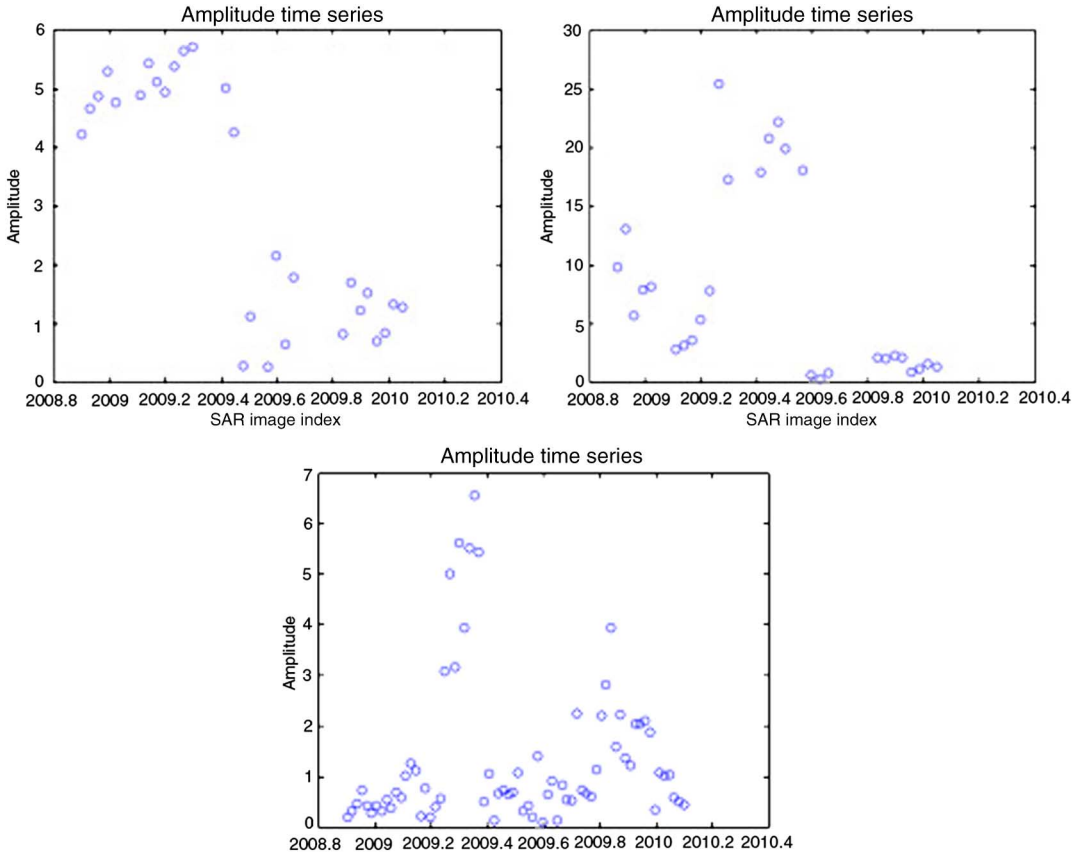

Fig. 1. Amplitude time series versus date for TerraSAR-X SAR data for three different cases of urban areas. Left: single transition, right: double transitions, and bottom: more than two transitions.

In order to test H_0, one can define a decision rule

$$\delta = \begin{cases} H_0, & F \leq c_\alpha \\ H_1, & F > c_\alpha \end{cases} \tag{4}$$

where $F_{K-1,N-K}(c_\alpha, \infty) = \alpha$, c_α is the threshold, and α is the level of significance.

The ANOVA is simply testing the ratio of the between groups and within groups. The term related with the difference of the group means named as the sum of squares between groups $\mathrm{SS}_{\mathrm{bg}}$ is the numerator of (3). Obviously, shall the $\mathrm{SS}_{\mathrm{bg}}$ is higher, it will be easier to separate the groups. The denominator of (3), called as sum of squares within groups, reflects the deviation of the single reflectivity values from the respective sample estimates.

Thus, the corresponding thresholding can be determined with the F distribution by $F_{K-1,N-K}$. We emphasize that (3) explicitly includes all the group relations in one expression and takes the advantage of fully exploiting the SAR amplitude series.

B. Localization of TI

The TI estimation technique can be derived by maximizing the F values. First, we assume the single transition case

$$\hat{i} = \mathrm{argmax}_{i=1,\ldots,N-2} \left(\frac{N-K}{K-1} \frac{\sum_{j=1}^{K} N_j (\mu_j - \mu)^2}{\sum_{i=1}^{K} \sum_{k=1}^{N} (I_{ik} - \mu_k)^2} \right) \tag{5}$$

where $K = 2$ for this case. In order to compute the mean of a group, we need at least two representatives of a group. This is why the initial value of i is one and the last value is $N-2$. Therefore, the argument that maximizes the F value will be the TI. For the case of multitransition, the instant computed through (5) shall be guaranteed to be the first one, so the probable following groups shall be disregarded. In order to overcome this problem, we assigned a guard that guarantees the number of pixels to generate a group. Hence, in this case, we have to write the same formula by

$$\hat{i} = \mathrm{argmax}_{i=1,\ldots,N-2} \times \left(\frac{t_i + D - 2}{2-1} \frac{\sum_{j=1}^{2} N_j (\mu_j - \mu)^2}{\sum_{i=1}^{t_i} (I_{i1} - \mu_1)^2 + \sum_{i=t_i+1}^{t_i+D} (I_{i2} - \mu_2)^2} \right) \tag{6}$$

where t_i is the TI and D is the guard. One can iteratively localize the TIs by reinitializing the index value $i = t_i + 1$ and the loop ends when the remained data are less than D. Here, we have to note that for each iteration, the F value shall be guaranteed to be higher than the previous one in order to avoid unnecessarily high number of groups. From another point of view, (6) represents an edge detector that the decision criterion is the maximization of the F value of the whole sequence.

It is interesting for this algorithm to analyze the no change case. In this case, the algorithm will force the data to have groups although there is no group. However, maximizing the F values does not generate a comparably high value to be assigned as a change, as the means of each group are close to each

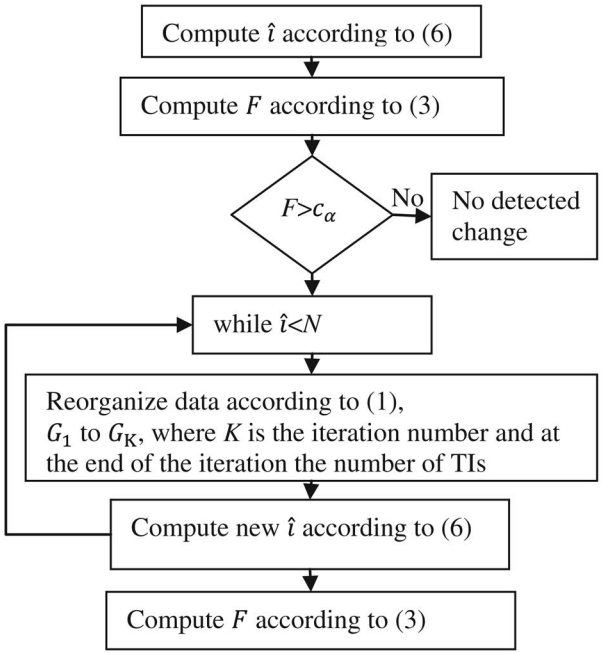

Fig. 2. Flow of the localization and F values computation.

other resulting in a lower $\mathrm{SS}_{\mathrm{bg}}$. The proposed methodology is given in Fig. 2.

C. Classification

The outputs of the proposed method are the F values and the TIs. Here, we propose three methods for the decision making: fully unsupervised thresholding of the F values, supervised thresholding of the F values, and classifying by giving the F values and the variance of the TIs as input to the SVM classifier.

First, under the assumption of F distribution of the ANOVA, one may explicitly compute a threshold c_α by defining a level of significance of $F_{K-1,N-K}(c_\alpha,\infty)=\alpha$. This approach is fully unsupervised. However, once the numbers of group members are not distributed homogenously, this method results in many false alarms. This is why we propose to apply a threshold for a probability of false alarm by selecting the "known to be unchanged regions," a supervised approach. Third, one may give F values as inputs to a state-of-the-art classifier, like SVM. In this section, we focused on the last one.

F values are discriminative features and can be obviously representative features for classification. One can use only these values for the classification procedure. However, in order to improve the performance of the proposed approach we preferred to use also the variance of TIs.

Till now, we only deal with the F value of a pixel, as a temporal approach and disregarded the relation of the pixel with its neighborhood. A spatio-temporal effort for the change detection purpose will have the opportunity to make a decision by taking into account the pixelwise and regionwise changes together. For the case of TerraSAR-X data that have a resolution of few meters or even one, it is more likely for an urban change to be observed in a region covering more than a single pixel. In our work, we took the advantage of spatial distribution of changes by considering the estimated TIs as a region is likely to have equal or close instants.

The plots of TIs show a regionwise homogeneity meaning a change at the same time in a region wider than a single pixel size. Therefore, the variance of these homogenous regions is lower than the unchanged regions. The idea simply means that the computed TIs are mostly close to each other for a changed region but is different for an unchanged region.

IV. Results

A. Data Set

Data used in this work were acquired by the TerraSAR-X sensor, collected between October 25, 2008 and February 5, 2012 for the area of interest in Hong Kong. The number of images is 70. The investigation was conducted at the site CUHK (Lat. 22.420'N, Long. 114.201'E).

B. Verification

In this section, a qualitative analysis is done in order to present the potentiality of the proposed method. For this reason, we first compared the Google Earth images that are acquired in 3 September 2008 and 12 June 2010, within an interval overlaps with the first half of the corresponding SAR data acquisition interval. These two images are shown in Fig. 3. In order to do further analysis, we had an onsite analysis to obtain the ground truth map shown in Fig. 4.

In Fig. 4, the regions that are rounded with the color yellow present the new roads, whereas the blue areas are construction sites where no complete buildings are observed at the last acquisition date of the Google Earth. The regions that are windowed or filled with black color are the changed areas. In the left, there is a black rectangle rounded by forest representing a house built inside the interval of SAR data acquisition. Also, the upper site of the image includes two newly built village houses. The black areas even inside the blue areas are the new buildings. The other black areas present a bridge over the road and the barriers on the road that are constructed during the SAR data acquisition.

It is a good exercise to evaluate the fully unsupervised automatic thresholding mechanism with the assumption of F distribution with the degrees of freedom K and $N-K$. Level of significance α is set to 0.95, and threshold is computed numerically by $F_{K-1,N-K}(c_\alpha,\infty)=\alpha$. This change detection image is extracted and overlaid on the Google Earth image in Fig. 5. In this figure, the background is seen for the areas below the threshold and blue is the lowest value of F, whereas red is the highest. As it is seen, the most of the scene is detected as changes, meaning a high false alarm rate. However, the F values are higher for the changed areas, like the buildings, whereas lower for the unchanged areas like the forest regions.

The false alarm rate for this case is observed to be relatively high. Especially for the cases that the number of group samples are not distributed homogenously, as it is also the case for the maximum-likelihood estimator [14], the F values can be still high although there is no significant difference.

In order to observe the supervised potentialities of the ANOVA, the F values are low pass filtered to lower the false alarms and manually thresholded to evaluate the performance

Fig. 3. Google Earth images of the site, acquired on 12 June 2010 and on 3 September 2008.

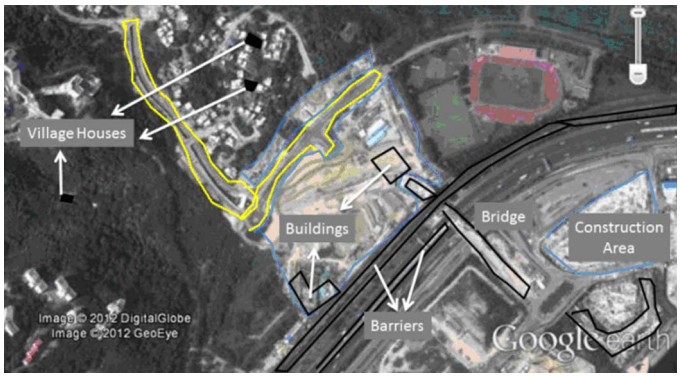

Fig. 4. Ground truth. Blue: construction area, yellow: roads, blacks: new buildings, a bridge over the road, and barriers on the road, and yellow: constructed roads.

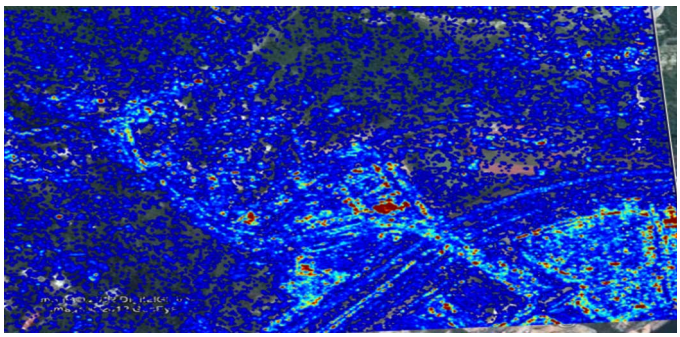

Fig. 5. F values are overlaid onto the Google Earth image by automatic thresholding the F values according to the distribution of F. Red is the highest and blue is the lowest. Google Earth image is seen for the regions that are lower than the threshold.

qualitatively. The threshold is determined by computing the distribution of the F values of a forest region that is known to be unchanged. For an unchanged region, the F value shall be lower. Hence, by determining 5% of probability of false alarm, the threshold is computed empirically. The resulting change detection map is overlaid on the Google Earth image and shown in Fig. 6. The blue regions in Fig. 5 are mostly disappeared and it is observed that for the forest area, where very little changes are known to be occurred, the manual thresholding promises a low false alarm rate. Also in this image, the new buildings that are shown in red regions in Fig. 4 are detected.

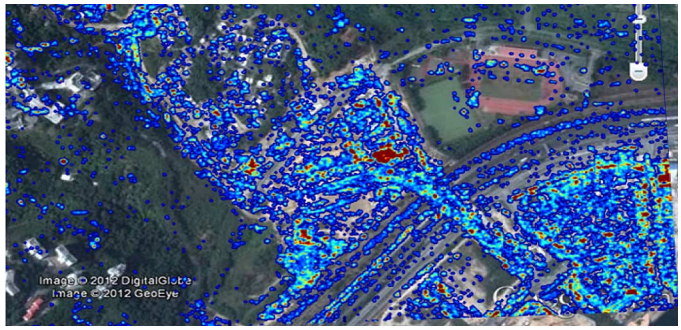

Fig. 6. F values are overlaid onto the Google Earth image by manual thresholding the F values. Red is the highest and blue is the lowest. Google Earth image is seen for the regions that are lower than the threshold.

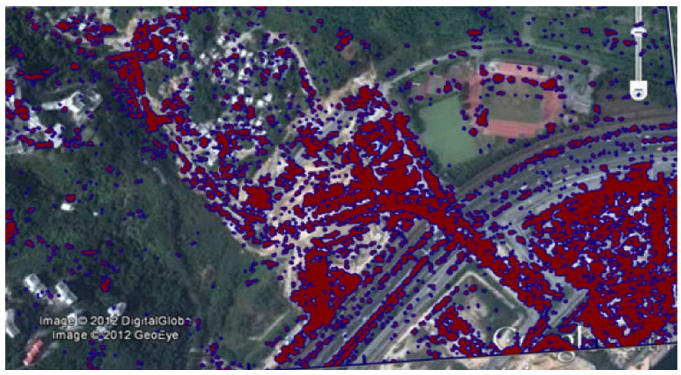

Fig. 7. Classified changes overlaid onto Google Earth image. Red regions are the detected changes. Google Earth image is seen for the regions that are detected as unchanged.

In the next experiment, the variance of the TIs and the F values are given as features to the support vector machines and classification is done by visually selecting a training set of 397 pixels labeled as change and 301 pixels labeled as no change. The visual selection procedure is achieved with the ground truth knowledge. A linear kernel is used for the SVM structure. One may use different classifiers, however, as the goal of this paper is to show the potentiality of the ANOVA, the performance of different classifiers are not compared. SAR data are trained with this sample set and the change detection map is extracted, as shown in Fig. 7. In this case, comparing with the manual thresholding, a better performance is obtained in terms of probability of detection. One may apply additional image morphology techniques like dilation for decreasing the false alarm rate. Another method is to apply erotion for increasing the probability of detection in order to improve the quality of this map.

We emphasize that the results in the previous three figures are maps, that once many SAR images are given as input, all the changes occurred at any time during the observation period is detected. Thus, there is no more a need to generate change detection maps for each image couples, but a single map for a series of a SAR image is already possible.

We have to also note that without time-series analysis, one must know the date of the change to select the suitable SAR images for the change detection map generation. The ANOVA can be applied to the series of SAR images without the preliminary knowledge on the ground truth, one can detect the changes.

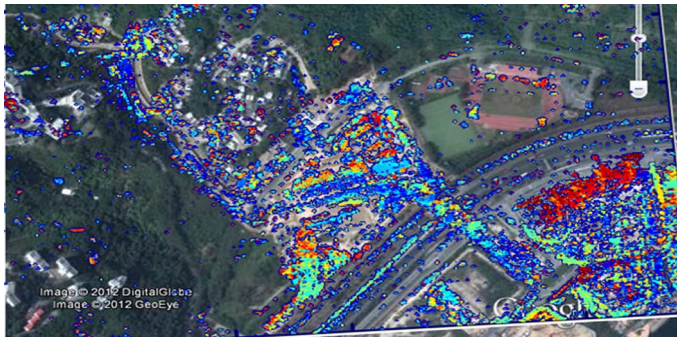

Fig. 8. SAR image index of the changed pixels. Blue: change occurred during 2008–2009. Red: change occurred during 2011–2012. Rest of the colors: change occurred between 2009 and 2011.

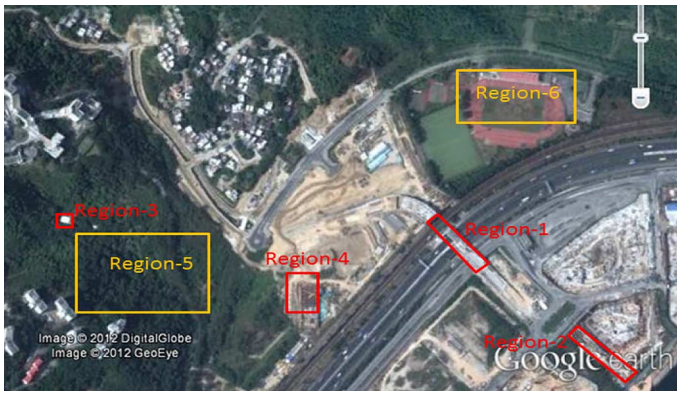

Fig. 9. Selected regions for validation. Red regions are the changed areas, whereas the orange ones are not changed areas.

In Fig. 8, the SAR image indexes, the first TIs, which are related with the acquisition dates of the data are presented. Also, this image shows that the TIs are likely to be homogenous for same regions, as an expectable result.

C. Validation

After the qualitative evaluation, more quantitative results by running three different experiments are given in this section. First, changed and unchanged regions are determined and the probability of detection and probability of false alarm is extracted for the manual thresholding and SVM cases. The automatic thresholding is disregarded as the false alarm rate which is too high. Second, the classification performance is assessed. Then another region of CUHK campus is studied for evaluating the small region detection performance. Third, the possible application of the proposed method, a land abuse case is presented.

1) CUHK Campus Experiment-1: In Fig. 9, four red windows present the changed areas, whereas the two orange ones are the unchanged regions. Region-1 is a bridge road that is constructed onto the highway. Regions-2–4 are the building areas. Region-5 is the forest area. The survey analysis also shows that this area still remains as forest, meaning no change inside the duration of SAR data acquisition. Region-6 is intentionally selected as a man-made structure including a building, a grandstand of a stadium to evaluate the algorithm robustness for the unchanged urban areas that have comparably higher intensities.

TABLE I
DETECTION PERFORMANCE OF CLASSIFIER, SVM, AND THE MANUAL THRESHOLDING. FIRST FOUR REGIONS SHOW THE PERFORMANCE OF DETECTION AND MISSED ONES. LAST TWO SHOWS THE PERFORMANCE OF FALSE ALARMS

Region class	Region no	No. of pixel	SVM, %	Manual thresholding, %
Changed regions	1	1274	78	87
	2	562	92	95
	3	25	100	96
	4	678	92	96
Unchanged regions	5	10871	8	10
	6	4714	5	6.5

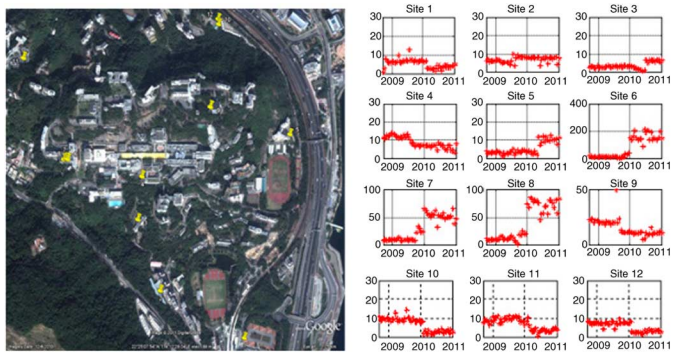

Fig. 10. Detected changes. Left: Google Earth image and right: amplitude time series.

The TIs are computed by maximizing the F values. The guard is selected as 3, meaning a group must be at least this amount of representatives. Increasing the guard region decreases the false alarm with the cost of poor probability of detection. Two experiments are done. First, the manual thresholding is evaluated in order to show the performance of the F values to represent the changes. Second, the SVM is utilized and those two are compared.

In Table I, the percentage of detection ratio is given. First, we emphasize that the values for the first four regions are the probability of detection, which are supposed to be high, whereas the last two are the probability of false alarm, which are supposed to be low. In order to assess the size of the region, the number of pixels of the corresponding regions is also given in Table I. For Region-1, a comparably lower detection ratio is extracted. The major reason of this case is probably that the region was before a highway and after a bridge road, those structures that backscattering is comparably lower resulting in a lower intensity. For Region-2, a good matching is seen to be extracted. Region-3 was a village house and all the pixels of the house are achieved to be classified as a change by SVM while manual thresholding misses one of the pixels. Region-4 has also good performance for both manual thresholding and SVM in terms of detection. For the last two regions, SVM and manual thresholding seem to have close and good results showing low false alarm rates.

In order to evaluate the performance of the classification, the labeled sample set is divided into two equal sized sets for training and test sets. These sample sets are visually classified. The randomly selected pixels are plotted and classified as change, no change, and unclassifieds. The SVM is first supervised with

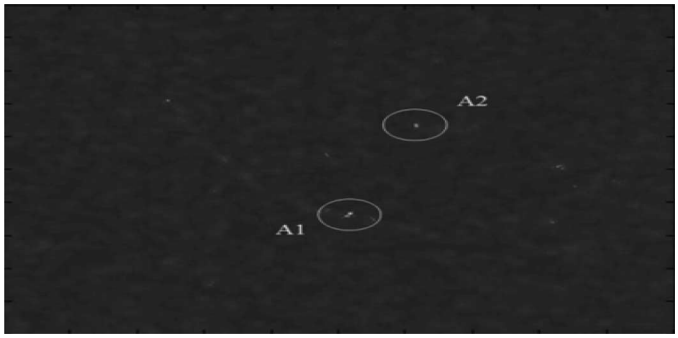

Fig. 11. CUHK campus. F values computed by ANOVA. The most significant spots are highlighted in white circles.

Fig. 13. Onsite survey of site A2.

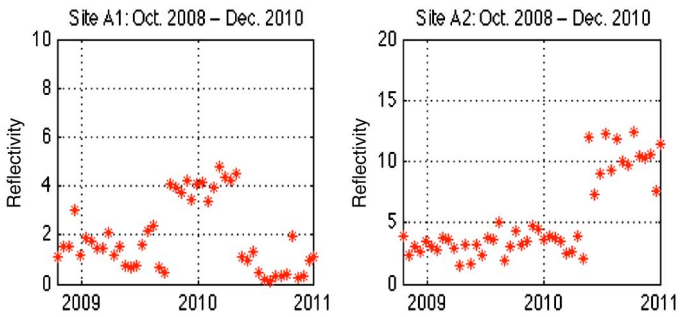

Fig. 12. Amplitude time series of site A1 and A2 versus date of data acquisition.

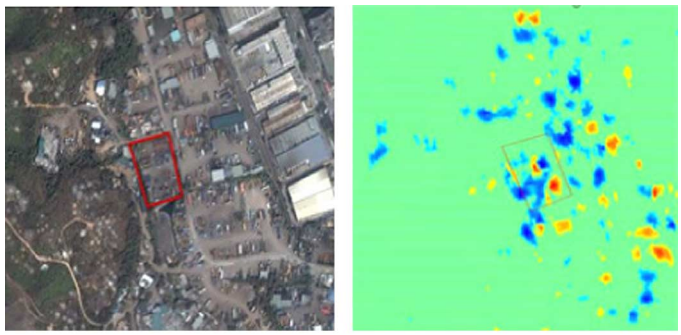

Fig. 14. (a) Birdview of the area of interest and (b) result of single pair comparison, red and yellow color: change in the recent image, blue: change in the previous image, and green: no change.

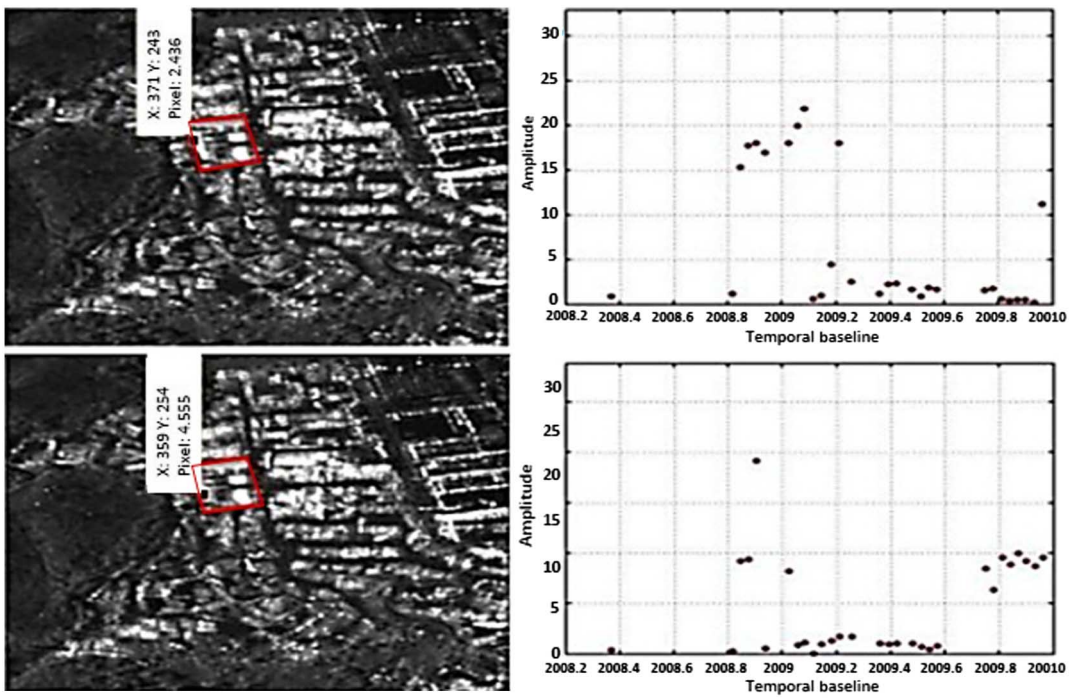

Fig. 15. Left: SAR image and right: amplitude time series of the selected pixel.

the training set and the tested with the remained. The test results show %1 false alarm, %90.32 right detections.

2) CUHK Campus Experiment-2: The second experiment is focused on smaller-sized urban changes, like Region-3 in Fig. 9. The major motivation behind is to assess the ANOVA performance alone for applications like land abuse which involves in a small region. Google Earth image of the application area is shown in the left of Fig. 10. The 12 yellow pins are the points of change and the right plots are the corresponding SAR amplitude series. SARPRoz [17] is used to handle and visualize data.

In Fig. 11, the F values are shown. The two points circled, shown as A1 and A2, are given more detailed attention and survey analysis is done.

In order to compute the probability of accepting H_0 hypothesis, an unchanged region is selected and the distribution of the F values is extracted. For site A1, the probability to accept H_0 hypothesis is as low as 6.22×10^{-7}, which strongly indicates that something changed in the site. However, the onsite survey failed in finding out any new structure in the location. By analyzing the time domain data (Fig. 12), it is observed that the amplitudes show a 2-step pattern with change dates of September 2009 and July 2010, meaning there was a temporal change that is no more valid. For site A2, the probability to accept H_0 hypothesis is 0.0011 meaning there is probably a change happened in site A2. Furthermore, in Fig. 12, it is shown that the time series shows a one step change in July 2010. An onsite survey of site A2 concluded an installation of a garbage bin as shown in Fig. 13.

3) Land Abuse Application: Another area of interest, where a change is known to be happened in October 2008, is cropped from the data for the purpose of change detection. The Google Earth view and the change detection map generated by simply Wiener filtering the difference of the images are shown in Fig. 14. There are change detection algorithms better than Wiener filtering; however, as the proposed work has no claim on a change detection algorithm for comparing two images, in order to show the difference image simply, this method is utilized. In Fig. 15, the SAR images and the corresponding time-series analysis are presented. According to this figure, this area, which is supposed to be an empty field, is concluded to be used illegally. Onsite observations show that the area is occupied by some containers. Therefore, it is presented that the time-series analysis change detection can be a good method for the application of land abuse detection.

V. Conclusion

In this work, the statistical method, named ANOVA, is applied for the multitemporal SAR data as a time-series analysis technique in order to detect the changes. Automatic and manual thresholding mechanisms and the classification performances show that the method has the potentiality to detect the multi-TIs and the possible changes given an amplitude time series as input. The validation and experimental results show that the proposed algorithm can achieve to provide a highly accurate change detection map of an area of interest. The change date and probability of detection are also the outputs of the algorithm. The application of the algorithm to the TerraSAR-X data of Hong Kong shows that the algorithm can provide promising applications for the CUHK campus and also for the land abuse detection. For the future works, an improvement on spatio-temporal analysis of the method and the automatic thresholding mechanism will be considered.

Acknowledgment

The authors would like to thank the Chinese University of Hong Kong for supporting the research, in particular the Institute of Space and Earth Information Science and its Director, Prof. Lin Hui.

References

[1] A. Singh, "Digital change detection techniques using remotely-sensed data," *Int. J. Remote Sens.*, vol. 10, pp. 989–1003, 1989.

[2] D. Lu *et al.*, "Change detection techniques," *Int. J. Remote Sens.*, vol. 25, no. 12, pp. 2365–2407, 2004.

[3] R. J. Dekker, "Speckle filtering in satellite SAR change detection imagery," *Int. J. Remote Sens.*, vol. 19, no. 6, pp. 1133–1146, 1998.

[4] Y. Bazi, L. Bruzzone, and F. Melgani, "An unsupervised approach based on the generalized Gaussian model to automatic change detection in multitemporal SAR images," *IEEE Trans. Geosci. Remote Sens.*, vol. 43, no. 4, pp. 874–887, Apr. 2005.

[5] Y. Bazi, L. Bruzzone, and F. Melgani, "Automatic identification of the number and values of decision thresholds in the log-ratio image for change detection in SAR images," *IEEE Geosci. Remote Sens. Lett.*, vol. 3, no. 3, pp. 349–353, Jul. 2006.

[6] C. Carincotte, S. Derrode, and S. Bourennane, "Unsupervised change detection on SAR images using fuzzy hidden Markov chains," *IEEE Trans. Geosci. Remote Sens.*, vol. 44, no. 2, pp. 432–441, Feb. 2006.

[7] F. Bovolo and L. Bruzzone, "A detail-preserving scale-driven approach to change detection in multitemporal SAR images," *IEEE Trans. Geosci. Remote Sens.*, vol. 43, no. 12, pp. 2963–2972, Dec. 2005.

[8] C. Carincotte, S. Derrode, and S. Bourennane, "Unsupervised change detection on SAR images using fuzzy hidden Markov chains," *IEEE Trans. Geosci. Remote Sens.*, vol. 44, no. 2, pp. 432–441, Feb. 2006.

[9] J. P. Qian *et al.*, "Applying an anomaly-detection algorithm for short-term land use and land cover change detection using time-series SAR images," *Giosci. Remote Sens.*, vol. 47, no. 3, pp. 379–397, 2010.

[10] G. Moser and S. B. Serpico, "Generalized minimum-error thresholding for unsupervised change detection from SAR amplitude imagery," *IEEE Trans. Geosci. Remote Sens.*, vol. 44, no. 10, pp. 2972–2982, Oct. 2006.

[11] E. Trouvé, Y. Chambenoit, N. Classeau, and P. Bolon, "Statistical and operational performance assessment of multitemporal SAR image filtering," *IEEE Trans. Geosci. Remote Sens.*, vol. 41, no. 11, pp. 2519–2530, Nov. 2003.

[12] C. Prati and F. Rocca, "Permanent scatterers in SAR interferometry," *IEEE Trans. Geosci. Remote Sens.*, vol. 39, no. 1, pp. 8–20, Jan. 2001.

[13] C. Colesanti, A. Ferretti, D. Perissin, C. Prati, and F. Rocca, *Evaluating the Effect of the Observation Time on the Distribution of SAR Permanent Scatterers*, Frascati, Italy: FRINGE, 2004.

[14] D. Perissin and A. Ferretti, "Urban target recognition by means of repeated spaceborne SAR images," *IEEE Trans. Geosci. Remote Sens.*, vol. 45, no. 12, pp. 4043–4058, Dec. 2007.

[15] F. Bujor, E. Trouvé, L. Valet, J. M. Nicolas, and J. P. Rudant, "Application of log-cumulants to the detection of spatiotemporal discontinuities in multitemporal SAR images," *IEEE Trans. Geosci. Remote Sens.*, vol. 42, no. 10, pp. 2073–2084, Oct. 2004.

[16] S. Hachicha, C. A. Deledalle, F. Chaabane, and F. Tupin, "Multi-temporal SAR classification according to change detection operators," *Analysis of Multi-temporal Remote Sensing Images (Multi-Temp), 2011 6th International Workshop*, Trento, July 12–14, 2011, pp. 133–136.

[17] D. Perissin, Z. Wang, and T. Wang, "The SARPROZ InSAR tool for urban subsidence/manmade structure stability monitoring in China," in *Proc. 34th Int. Symp. Remote Sens. Environ.* (ISRSE), Syndey, Australia, Jan. 2011.

[18] P. Lombardo and T. M. Pellizzeri, "Localization of step changes in multitemporal SAR images," *IEEE Trans. Aerosp. Electron. Syst.*, vol. 38, no. 4, pp. 1256–1275, Oct. 2002.

[19] P. Lombardo and T. M. Pellizzeri, "Maximum likelihood signal processing techniques to detect a step pattern of change in multitemporal SAR images," *IEEE Trans. Geosci. Remote Sens.*, vol. 40, no. 4, pp. 853–870, Apr. 2002.

[20] M. Santoro, J. E. S. Fransson, L E. B. Eriksson, and L. M. H. Ulander, "Clear-cut detection in swedish boreal forest using multi-temporal ALOS PALSAR backscatter data," *IEEE J. Sel. Top. Appl. Earth Observ. Remote Sens.*, vol. 3, no. 4, pp. 618–631, Dec. 2010.

Ozan Dogan was born in Turkey, in 1979. He received the B.Sc. degree in electronics and telecommunication engineering, the M.Sc. and Ph.D. degrees in satellite communication and remote sensing technologies, both in Istanbul Technical University (ITU), Istanbul, Turkey, in 2002, 2004, and 2011, respectively.

He worked as a Research Assistant in ITU (2002–2005), System Engineer in MilSOFT (2005–2007), System Engineer in SDT (2007–2011), Postdoc Fellow in CUHK (2012), Senior System Engineer in Meteksan (2013). He is now with Ortana as an R&D Team Leader. Since 2002, he focused on radar signal processing, published many papers, and also worked as a Developer in many radar-related projects, including SAR image processing, SAR signal processing, multitemporal SAR change detection, millimeter wave technologies, and traffic radars.

Daniele Perissin was born in Milan, Italy, in 1977. He received the M.Sc. degree in telecommunications engineering and the Ph.D. degree in information technology (cum laude) from Politecnico di Milano, Milano, Italy, in 2002 and 2006, respectively.

He joined the Signal Processing Research Group at Politecnico di Milano in 2002, and since then, he has been working on the permanent scatterers technique in the framework of radar remote sensing. In 2009, he joined as a Research Assistant Professor with the Institute of Space and Earth Information Science, Chinese University of Hong Kong, Hong Kong, China. Since October 2013, he holds a position as Assistant Professor at Purdue University, School of Civil Engineering, West Lafayette, IN, USA. He is author of a patent on the use of urban dihedral reflectors for combining multi-sensor Interferometric Synthetic Aperture Radar (InSAR) data and has published about 80 research works in journals and conference proceedings. He is the Developer of the software Sarproz for processing multi-temporal InSAR data.

Dr. Perissin received the JSTARS best paper award in 2012.